

ELECTRONIC SUPPLEMENTARY INFORMATION (ESI)

Naringin ameliorates radiation-induced hepatic damage through modulation of Nrf2 and NF- κ B pathways

Krishnendu Manna¹, Amitava Khan¹, Sushobhan Biswas¹, Ujjal Das¹, Aaveri Sengupta¹, Dipanwita Mukherjee², Anindita Chakraborty², Sanjit Dey^{1*}

(Figure: S1, S2, S3, S4, S5, S6, S7)

Materials and methods:

Scanning electron microscopic assessment:

Briefly liver tissues were washed properly and initially fixed with neutral formalin buffer. Then the tissue was again fixed in 2.5% glutaraldehyde and incubated with 1% osmium tetroxide for 2 hr. Then the tissues were dehydrated in a graded series of ethanol solutions, dried in a critical point drying apparatus (Quorum Technologies) by liquid carbon dioxide, mounted on aluminum stubs, and vacuum coated with gold palladium (Polaron SC 7620). Coated specimens were then viewed in a scanning electron microscope (ZEISS EVO-MA 10, Jena, Germany) and maximum damaged areas were photographed ¹.

Histopathological assessment:

The standard histopathological gradations were followed - Grade 0: normal histology; Grade 1: presence of degenerated hepatocytes with only rare foci of necrosis; Grade 2: mild centrilobular necrosis around the central vein, occupying only a part of Rappaport's zone; Grade 3: established necrosis limited to zone; and Grade 4: extensive, confluent centrilobular necrosis involving Rappaport's zone.

Assessment of DNA damage using comet assay:

The assay was taken from the protocol described previously ². After harvesting the cell (2×10^6 cells/dish in a 65-cm dish) were suspended in 1% low-melting-point agarose in PBS (pH 7.4) and pipetted onto super frosted glass microscope slides precoated with a layer of 1% normal-melting-point agarose. Then the slides were immersed in lysis solution [2.5 M NaCl, 100 mM EDTA, 10 mM Tris (pH 10.0), and 1% Triton X-100] at 4°C for 1 h to remove the cellular proteins and placed in a horizontal electrophoresis tank containing alkaline buffer (300 mM NaOH, 1 mM EDTA pH 13.0) at 4°C for 20 min to allow the separation of the two DNA strands (alkaline unwinding). Electrophoresis was performed in the unwinding solution [3 V (1 V/cm) and 300 mA] for 15 min. The slides were then washed and stained with PI (2.5 µg/ml). The PI-stained nucleus was examined under a fluorescence microscope at a 400× magnification. The damage was not homogeneous, and the visual scoring of the cellular DNA on each slide was based on the characterization of 100 randomly selected nuclei.

Results:

ESI1. NG restored IR-induced hepatic ultrastructural alteration:

To understand IR-induced ultrastructural changes in murine liver, scanning electron microscopy (SEM) was carried out. Well maintained tissue architecture was found in control and NG pretreated mice. Images also revealed that the external membrane of the liver showed a regular lobular architecture with no signs of surface morphological changes (**Fig. S1A and S1C**). Irradiated liver showed marked changes in the surface morphology, shrinkage and appeared to have variously-shaped aggregated tissue granules with a few major pores. External tissue inflammation was also noted in certain areas (**Fig. S1B**). However, NG pretreatment in IR group revealed some elongated structure in the membrane but no sign of the membrane aggregation and shrinkage (**Fig. S1D**).

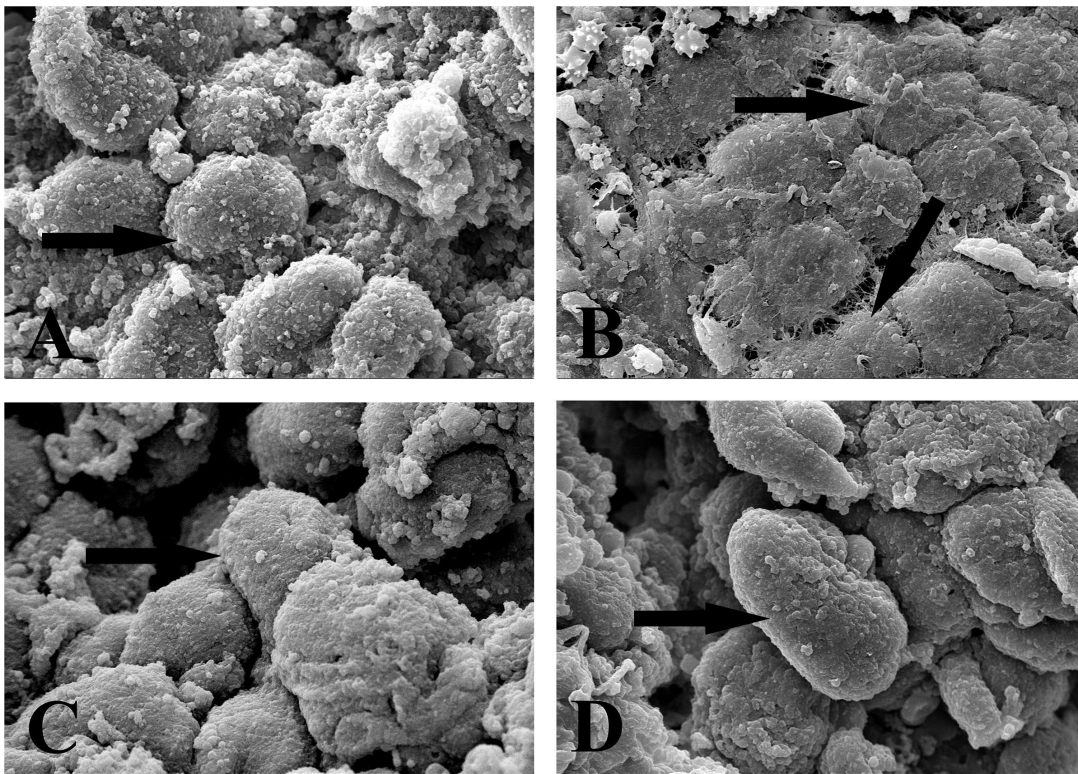


Fig. S1. Ultra-structural changes of liver from various treated group evaluated by scanning electron microscopy. Images are represented as (A) Control (B) Irradiated with 6 Gy IR (C) NG (75 mg/kg) pretreated (D) NG (75 mg/kg) pretreated before IR (6 Gy). Five fields were examined per slide; five slides were examined per group. Magnification of scanning electron microscopic images was 5.00K \times .

ESI2. NG protected IR-induced nuclear DNA damage:

To investigate the effect of NG on IR-induced DNA damage, comet assay was performed (**Fig. S2A, S2B, S2C and S2D**). The comet assay is a sensitive assay to detect IR-induced DNA damage, such as strand breaks and the formation of alkali-labile sites. The alteration of comet attributes of hepatic cells upon different treatments is presented in **Fig. S2E, S2F, S2G, S2H, S2I and S2J**.

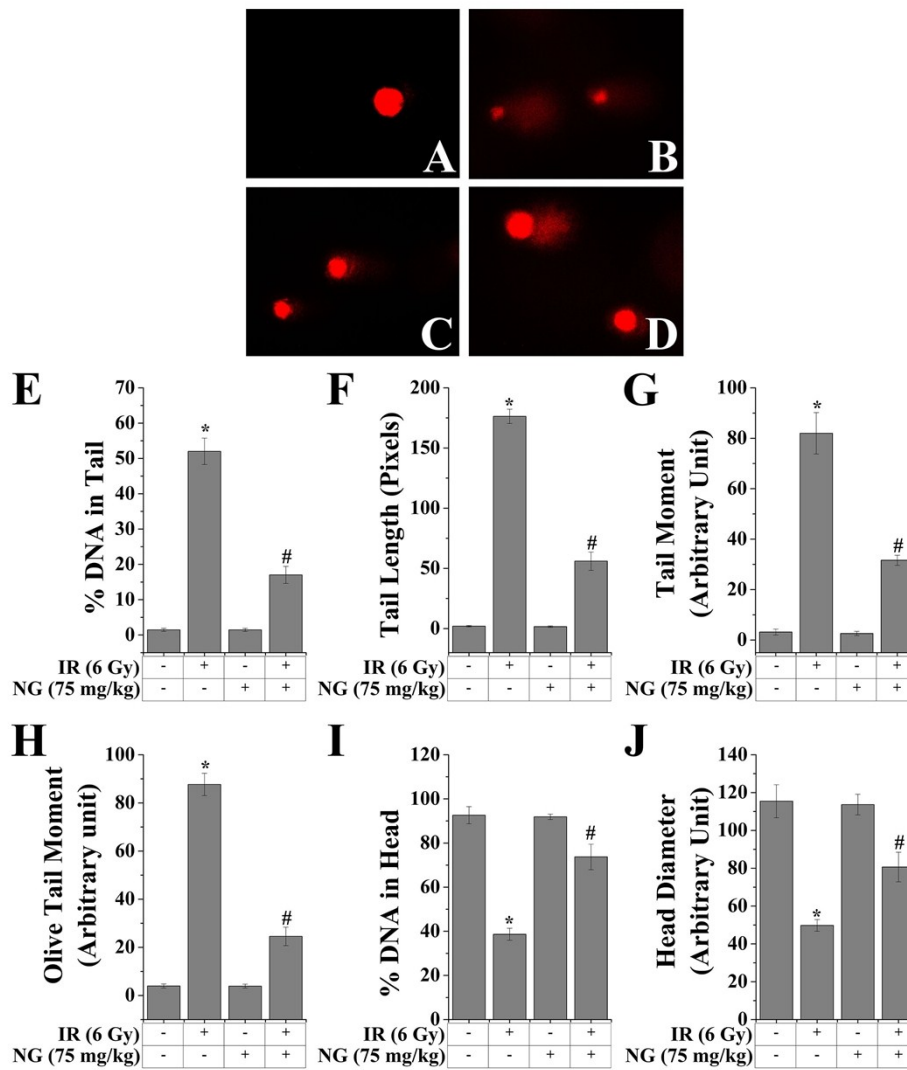


Fig. S2. Assessment of nuclear DNA damage after the treatment of NG (75 mg/kg) and 6 Gy IR. Comet photographs showing (A) Control (B) 6 Gy irradiated (C) NG (75 mg/kg) pretreated and (D) NG pretreated (75 mg/kg) prior to 6 Gy irradiated hepatocytes. Photographs were analyzed by Comet Score Software. Graphs represented as (E) % DNA in Tail (F) Tail Length (G) Tail Moment (H) Olive Tail Moment (I) % DNA in Head (J) Head Diameter. Values are presented as mean \pm SEM (n=5). p<0.05 was

considered as significant. Statistical comparison: *Control vs. IR (6 Gy); #IR (6 Gy) vs. NG (75 mg/kg) + IR (6 Gy).

A significant ($p < 0.05$) increase in tail length (88.17-fold), tail moment (25.97-fold), olive tail moment (22.22-fold), % DNA in tail (35.63-fold) and a significant decrease in % DNA in head (0.42-fold), head diameter (0.43-fold) was found in IR-treated group when compared to the control group. On the other hand, NG (75 mg/kg) pre-administration significantly ($p < 0.05$) modulated the IR-induced nuclear DNA damage by altering the levels of comet attributes (28-fold for tail length, 10.02-fold for tail moment, 6.23-fold for olive tail moment, 11.66-fold for % DNA in tail, 0.80-fold for % DNA in head and 0.70-fold for head diameter). Further, there was no significant increase in the comet formation (0.83-fold for tail length, 0.82-fold for tail moment, 0.99-fold for olive tail moment, 0.99-fold for % DNA in tail, 0.99-fold for % DNA in head and 0.98-fold for head diameter) in the NG-pretreated group alone when compared to the control group.

ESI3. NG attenuated IR-induced loss of mitochondrial transmembrane potential (MMP):

MMP was found to be reduced rapidly, when mice were exposed to 6 Gy IR, which was detected by a weakening of fluorescence intensity of a mitochondrial fluorescence probe, Rhodamine-123 (**Fig. S3A and S3B**). As compared to the control cells, IR-treatment decreased the Rhodamine-123 fluorescence intensity. However, pretreatment with NG (75 mg/kg) significantly enhanced the Rhodamine-123 fluorescence intensity, suggesting its involvement on the normalization mitochondrial membrane potential.

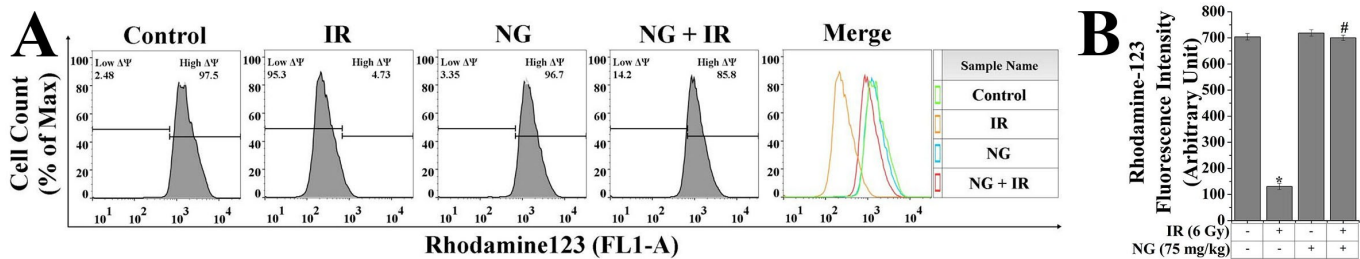


Fig. S3. (A) Histogram showing mitochondrial membrane potential change using Rhodamine-123 (B) Quantitative analysis of Rhodamine-123 fluorescence intensity. Values are presented as mean ± SEM

(n=5). $p < 0.05$ was considered as significant. Statistical comparison: *Control vs. IR (6 Gy); #IR (6 Gy) vs. NG (75 mg/kg) + IR (6 Gy).

ESI4. NG inhibited IR-induced phosphorylation of p50 (NF- κ B):

Activation of NF- κ B was based on the detection of its translocation into the nuclei from its initial localization in the cytoplasm where it exists in an inactive form. p50, an important sub-unit of NF- κ B, was significantly phosphorylated with the exposure of IR. However, this phosphorylation markedly inhibited with the pretreatment of NG (Fig. S4A and S4B).

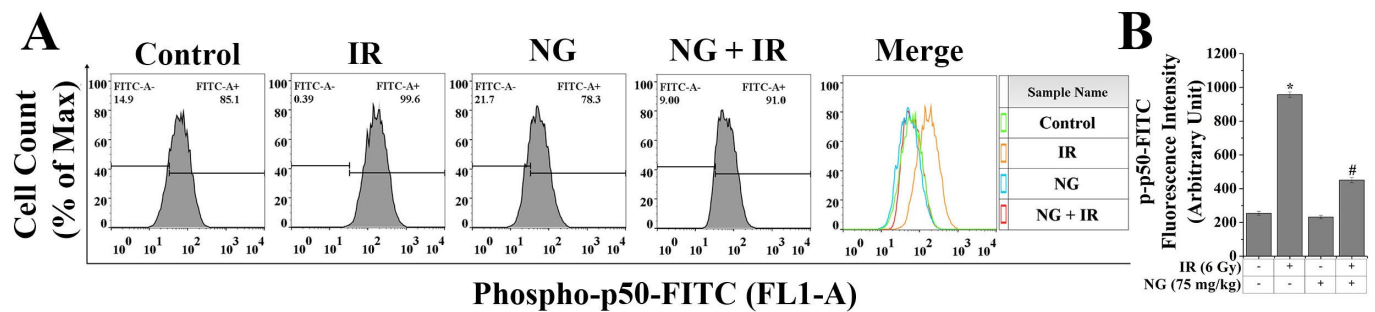


Fig. S4. Assessment of IR-induced NF- κ B pathway activation and its prevention by the pretreatment of NG. (A) Flow cytometric histogram showing phosphorylated expression of p50 (B) Bar graph showing relative fluorescence intensity of p-p50-FITC. Values are presented as mean \pm SEM (n=5). $p < 0.05$ was considered as significant. Statistical comparison: *Control vs. IR (6 Gy); #IR (6 Gy) vs. NG (75 mg/kg) + IR (6 Gy)

ESI5. NG modulated IR-induced nuclear localization of p65 (NF- κ B) and Nrf2:

Consistent with the protein expression, a significant modulatory effect of NG on the IR-induced p65 and Nrf2 nuclear translocation was determined by immunofluorescence staining. As shown in Fig. S5A, the fluorescence intensity of p65-FITC in the nuclear area was significantly increased and Nrf2-FITC was decreased in hepatic tissue treated with irradiation as observed from the intensity curve (Fig. S5B, S5C, S5D and S5E). However, concurrent treatment with NG and IR significantly modulated the increase in p65-FITC fluorescence as well as decrease in Nrf2-FITC fluorescence over the IR group. Only NG pretreated group did not show significant nuclear localization of p65 in terms of p-p65-FITC fluorescence

over the control group. In contrast, NG pretreated group markedly enhanced the Nrf2-FITC fluorescence when compared to the control group.

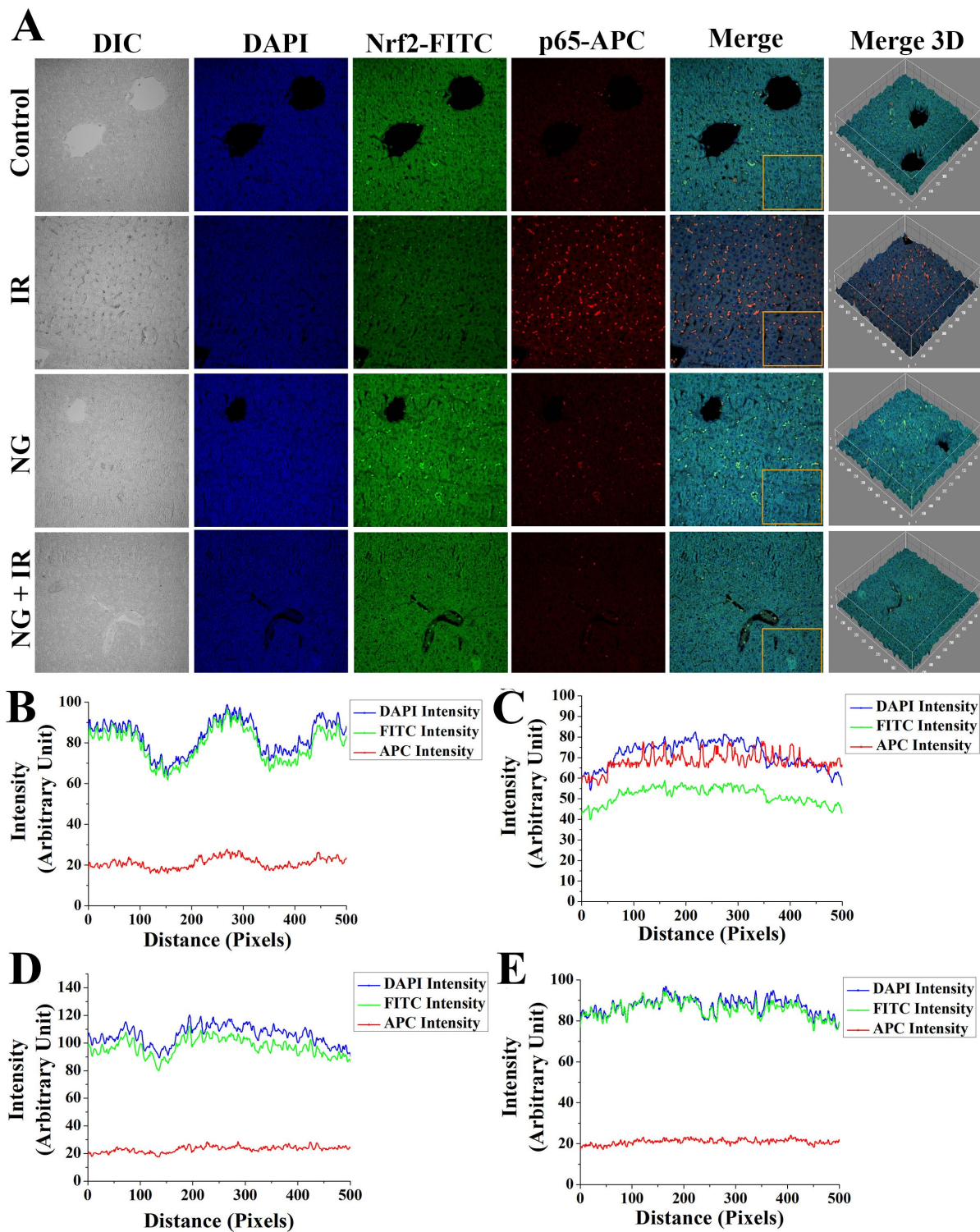


Fig. S5. (A) Immunofluorescence images showing the expression of Nrf2 and p65. Slides were viewed using confocal microscopy (Magnification 200 \times). Intensity analysis of relative fluorescence of Nrf2-

FITC, p65-APC and DAPI. Intensity analyses were done using Image J software from the respective immunofluorescence micrographs. Graph showing (B) Control (C) IR-treated (6 Gy) (D) NG pretreated (75 mg/kg) (E) NG pretreated (75 mg/kg) prior to IR (6 Gy).

ESI6. NG reduced IR-induced elevation of COX-2:

Immunofluorescence analysis was revealed that the relative COX-2-FITC fluorescence intensity markedly increased in the IR group in comparison to the control and NG pretreated group. Furthermore, NG pretreatment showed a significant ($p < 0.05$) decrease in COX-2-FITC fluorescence intensity over the IR group (**Fig. S6**). Similar kind of result was also found in immunoblot analysis.

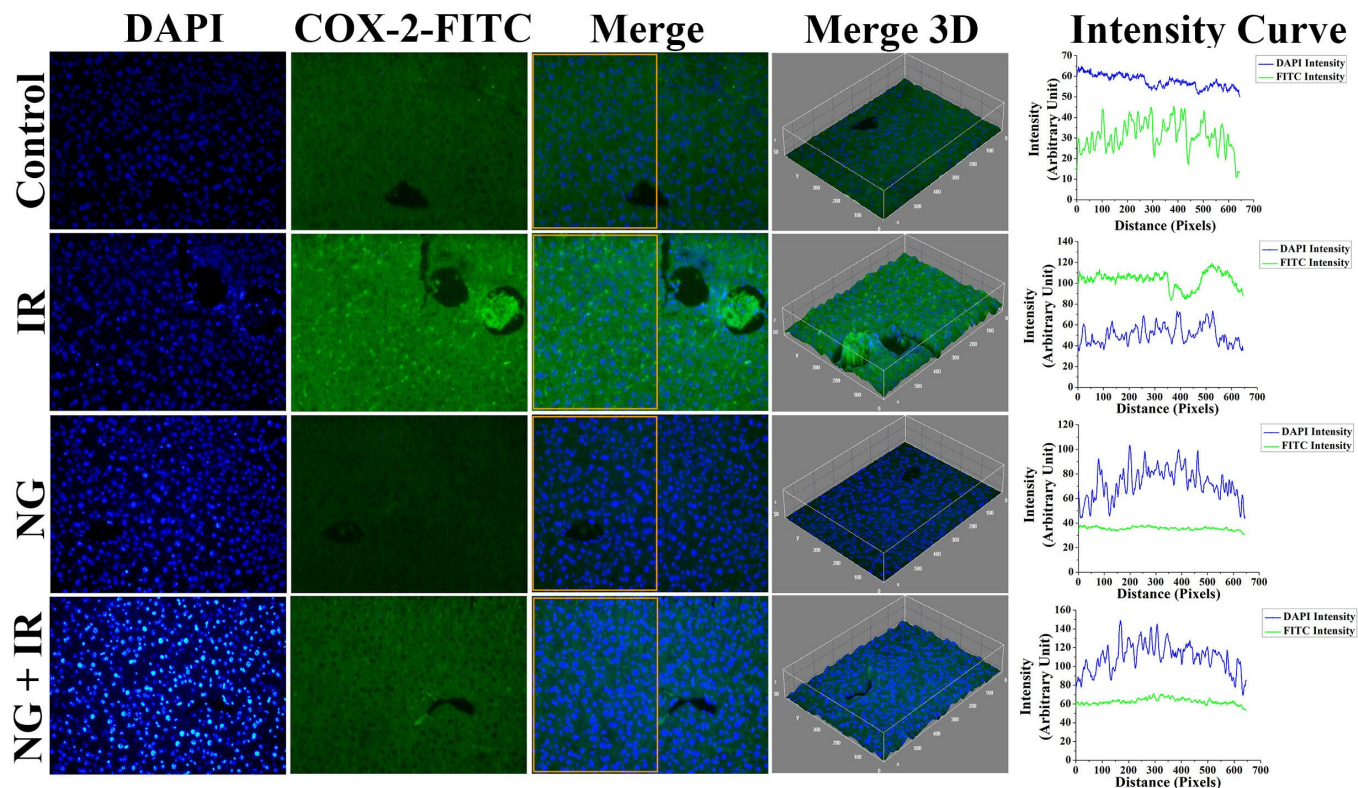


Fig. S6. Immunofluorescence images showing qualitative expression of COX-2. Slides were viewed using fluorescence microscopy (Magnification 200×). Intensity analysis of relative fluorescence of COX-2-FITC and DAPI. Intensity analyses were done using Image J software from the respective immunofluorescence micrographs.

ESI7. NG enhanced IR-induced depletion of Mn-SOD:

Fig. S7 showed that Mn-SOD expression was markedly decreased (0.73-fold) in the IR group when compared to the control group. NG pretreatment enhanced this level (0.98-fold) towards normal level in the irradiated group (**Fig. S7A and S7B**).

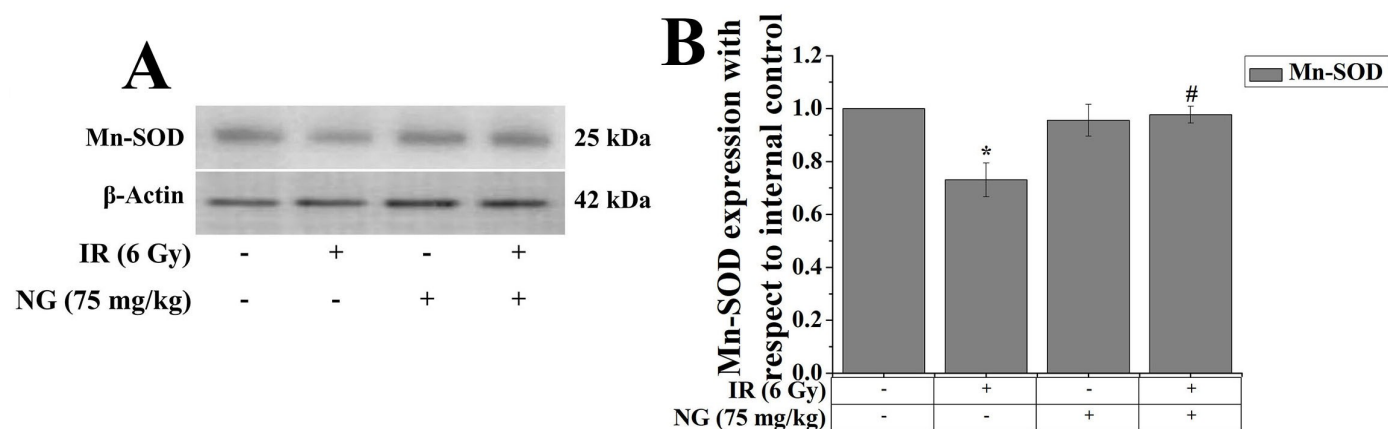


Fig. S7. (A) Representative immunoblot of Mn-SOD (B) Densitometric analysis of relative protein expression of Mn-SOD. β -Actin was served as internal control. Values are presented as mean \pm SEM (n=5). $p < 0.05$ was considered as significant. Statistical comparison: *Control vs. IR (6 Gy); #IR (6 Gy) vs. NG (75 mg/kg) + IR (6 Gy).

Reference:

1. N. Chatterjee, S. Das, D. Bose, S. Banerjee, T. Jha and K. D. Saha, *Toxicol. Lett.*, 2015, 232, 499-512.
2. E. Diem, S. Ivancsits and H. W. Rudiger, *J. Toxicol. Environ. Health A*, 2002, 65, 641-648.